THE ASTROPHYSICAL JOURNAL, 402:271–279, 1993 January 1

PARTICLE ACCELERATION AND NONTHERMAL RADIO EMISSION IN BINARIES OF EARLY-TYPE STARS

D. EICHLER
Physics Department, Ben-Gurion University, Beer Sheva, 84105, Israel
AND
V. USOV
Physics Department, Weizmann Institute, Rehovot 76100, Israel
Received 1992 April 2; accepted 1992 July 13

ABSTRACT

It is shown that the stellar wind collisions in early-type binaries may be strong sources of both high-energy particles and nonthermal emission. Nonthermal radio emission may be observed only if the orbital period of the binary is more than some critical value. For a typical Wolf-Rayet binary the value of the critical period is of the order of a month when the frequency of observation is a few GHz. Observations of nonthermal radio emission of the remarkable Wolf-Rayet binary WR 140, such as luminosity, spectrum, time variability in the process of orbital motion, the size of nonthermal radio source, etc., are explained by a model in which its nonthermal radio emission is generated at the site of stellar wind collision. Considerations of shock acceleration theory suggest that the WR 140 system may be a strong source of γ-rays. It is proposed that *EGRET* could both measure the time dependence of the γ-ray emission as well as resolve an inverse Compton spectrum from a pion decay spectrum and thereby provide information on the electron versus proton content of the relativistic particles.

Subject headings: acceleration of particles — radio continuum: stars — stars: early-type — stars: mass loss — stars: Wolf-Rayet

1. INTRODUCTION

Early-type stars, specifically OB stars and Wolf-Rayet (WR) stars, are strong sources of both thermal and nonthermal radio emission (Florkowski & Gottesman 1977; Dickel, Habing, & Isaacsman 1980; Hogg 1982; Felli & Panagia 1982; Abbott et al. 1986; Bieging, Abbott, & Churchwell 1989; Felli & Massi 1991). All early-type stars possess strong stellar winds (e.g., Conti 1978), and the thermal radio emission is naturally explained as free-free emission from the extended envelopes formed by the mass loss (Wright & Barlow 1975; Panagia & Felli 1975). White & Becker (1982, 1983) and Hogg (1985) have confirmed this thermal wind model in the stars P Cyg, Cyg OB2 No. 12, and γ^2 Vel by resolving the sources of radio emission with the VLA. The nature of the nonthermal radio emission is unknown, although it is probably synchrotron emission.

Particle acceleration and nonthermal emission from unsteady dense winds of single stars has been discussed by White (1985) and Chen & White (1991). Volk & Biermann (1988) have considered acceleration at the termination shocks of such winds.

The early-type stars (AS 431, HD 168112, HD 167971, HD 193793, Cyg OB2 No. 9, Cyg OB2 No. 8A, etc.) which are the most powerful sources of nonthermal radio emission also have anomalous strong X-ray emission (Pollock 1987; Chlebowski, Harnden, & Sciortino 1989). The X-ray luminosity of early-type stars is dependent on whether or not they belong to a binary system. Massive binaries of early-type stars are on average much brighter in X-rays than single stars (Pollock 1987; Chlebowski 1989). The additional X-ray component of massive binaries results from stellar wind collision in these systems (Prilutskii & Usov 1975, 1976; Moffatt et al. 1982; Pollock 1987; Chlebowski 1989; Luo, McCray, & Mac Low 1990; Usov 1992a). The correlation between nonthermal radio and enhanced X-ray fluxes point to their common origin (Chlebowski 1989). Therefore, most probably, the acceleration of the relativistic electrons required to account for the synchrotron radio emission is also a consequence of the collision of the two stellar winds. Williams, van der Hucht, & Thé (1987) and Williams et al. (1990) arrived at the same conclusion about the origin of the relativistic electrons generating the nonthermal radio emission of binary HD 193793 (WR 140) from the analysis of time variations of the radio emission. Below, particle acceleration and the generation of nonthermal radio emission in the region of stellar wind collision in the WR + OB binaries are considered. However, the main results of this consideration are applicable not only for the WR + OB binaries but also for any massive binary only if the assumptions we use about the parameters of binary and stellar winds are valid.

Typical parameters of stellar winds, geometry of the region of stellar wind collision, and the properties of the magnetic field in this region are discussed in § 2. Particle acceleration near the shocks and generation of nonthermal radio emission are described in § 3. The structure of radio sources in massive binaries and expected time variations of nonthermal radio emission in the process of orbital rotation are considered in § 4. The interpretation of observational data and some theoretical predictions on the nonthermal radio and γ-ray emission from the remarkable massive binary WR 140 are given in § 5. The discussion and summary are presented in § 6.

2. STELLAR WIND COLLISION IN WR + OB BINARY

2.1. *Stellar Wind Parameters*

As a class, WR stars have the highest known mass fluxes of any stellar type (Abbott & Conti 1987). The mass-loss rate for WR stars, M_{WR}, and the terminal velocity of the matter

outflow, V_{WR}^{∞}, far from the star amount to $\sim(0.8\text{–}8) \times 10^{-5}$ $M_{\odot}$ yr^{-1} and $\sim(1\text{–}5) \times 10^{3}$ km s^{-1}, respectively (Willis 1982; Abbott et al. 1986; Torres, Conti, & Massey 1986). OB stars also have an intense stellar wind: $\dot{M}_{OB} \sim 10^{-6}$ $M_{\odot}$ yr^{-1}, $V_{OB}^{\infty} \sim (1\text{–}3) \times 10^{3}$ km s^{-1} (Garmany & Conti 1984; Leitherer 1988).

For a typical WR + OB binary ($\dot{M}_{WR} \simeq 2 \times 10^{-5}$ $M_{\odot}$ yr^{-1}, $\dot{M}_{OB} \simeq 10^{-6}$ $M_{\odot}$ yr^{-1}, $V_{WR}^{\infty} \simeq V_{OB}^{\infty} \simeq 2 \times 10^{3}$ km s^{-1}, the distance between the components of binary $D \simeq 10^{13}$ cm, the stellar wind gas temperature $T \simeq 4 \times 10^{4}$ K) the parameters of the gas ahead of the region of stellar wind collision will be the following: the gas density $\rho \simeq 10^{-14}$ g cm^{-3}, the sound speed $V_s \simeq 10$ km s^{-1} and the Mach number $\mathcal{M} = V_{WR}^{\infty}/V_s \simeq 2 \times 10^{2}$. The gas outflow from early-type stars is supersonic ($\mathcal{M} \gg 1$).

2.2. *Geometry of the Region of Stellar Wind Collision*

The winds from the binary components flow nearly radially out to the shocks (see Fig 1). In the shock the gas is heated to temperature $\sim 10^{7}$ K and generates X-ray emission (Prilutskii & Usov 1975, 1976; Luo et al. 1990; Stevens, Blondin, & Pollock 1992; Usov 1992a) discussed in § 1. Behind the shock the hot gas outflows from the region of stellar wind collision nearly along the contact surface (see in detail Usov 1992a).

In the case of the collision of two spherical winds the distances r_{WR} and r_{OB} from WR or OB stars, respectively, to the region where these winds meet is

$$r_{WR} = \frac{1}{1+\eta^{1/2}} D, \quad r_{OB} = \frac{\eta^{1/2}}{1+\eta^{1/2}} D \tag{1}$$

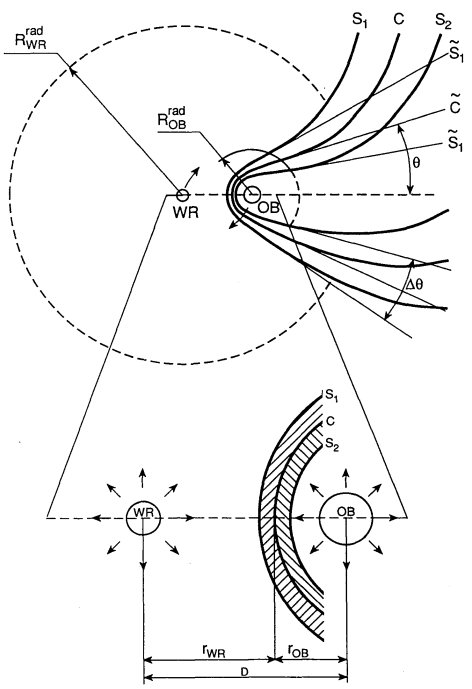

FIG. 1.—Collision of two stellar winds in the WR + OB binary. S_1 and S_2 denote the shock waves and C is the contact surface. The surfaces S_1, S_2, and C are near the conic surfaces $\tilde{S}_1$, $\tilde{S}_2$, and $\tilde{C}$, respectively, at intermediate distances $[r_{OB} \ll r \ll (P/2)V_{WR}^{\infty}]$ from the OB star. R_{WR}^{rad} and R_{OB}^{rad} are the radii of the radio photosphere for the WR and OB stars. The directions of the orbital motion of the binary components are shown by the arrows. The region of stellar wind collision is hatched at the lower part of the figure at which the collision region is enlarged.

(see Fig. 1), where

$$\eta = \frac{\dot{M}_{OB} V_{OB}^{\infty}}{\dot{M}_{WR} V_{WR}^{\infty}} .$$

Since $\dot{M}_{OB} \sim (0.01\text{–}0.1)\dot{M}_{WR}$ and $V_{OB}^{\infty} \sim V_{WR}^{\infty}$, the dimensionless parameter η is small ($\eta \ll 1$). Hence, the region of stellar wind collision is much nearer to the OB star than to the WR star ($r_{WR} \gg r_{OB}$).

The form of the contact surface C near the OB star ($r \sim r_{OB}$) is given by

$$|\boldsymbol{R}_c(\chi)| \simeq r_{OB} \frac{\chi}{\sin \chi} \tag{2}$$

for $\chi \lesssim \pi/2$ [here χ is the angle between the radius vector $\boldsymbol{R}_c(\chi)$ from the center of the OB star to the point at the contact surface and the line connecting the components of the binary].

At intermediate distances $[r_{OB} \ll r < (P/2)V_{WR}^{\infty}]$ from the OB star the contact surface C approaches the conic surface $\tilde{C}$ with angle θ (see Fig. 1). The value of θ was calculated numerically by Girard & Willson (1987). The results of the calculations may be approximated by the following analytic equation (L. M. Ozernoy 1991, private communication)

$$\theta \simeq 2.1\left(1 - \frac{\eta^{2/5}}{4}\right)\eta^{1/3} \quad \text{for } 10^{-4} \le \eta \le 1 \tag{3}$$

with accuracy $\sim 1\%$.

The shock fronts S_1 and S_2 are near the conic surfaces $\tilde{S}_1$ and $\tilde{S}_2$ at $r_{OB} \ll r < (P/2)V_{WR}^{\infty}$ as well. In the case of wide WR + OB binaries, like WR 140, when the fraction of the thermal energy of the hot gas lost by emission in the shock layers is small the angle $\Delta\theta$ between these conic surfaces is $\sim\theta$ (Lebedev & Myasnikov 1988). In the other case the value of $\Delta\theta$ is smaller than θ and asymptotically approaches zero if this fraction goes to unity.

The contact surface C and two shock fronts S_1 and S_2 are twisted at a distance more than $\sim(P/2)V_{WR}^{\infty}$ due to the orbital rotation and have a spiral form (see Fig. 1). Since the orbital velocities in massive binaries are typically much smaller than the terminal velocities, we have $(P/2)V_{WR}^{\infty} \gg D$.

2.3. *The Strength of Magnetic Field near the Region of Stellar Wind Collision*

Let us assume that the external magnetic field of the star without stellar wind is dipole; then in the case of gas outflow from the star the strength of the magnetic field and its geometry in the outflowing gas is (Weber & Davis 1967; Usov & Melrose 1992)

$$B \approx B^{s} \times \begin{cases} \left(\dfrac{R}{r}\right)^{3} & \text{for } R \le r < r_A \text{ (dipole)}, \\ \dfrac{R^3}{r_A r^2} & \text{for } r_A < r < R\dfrac{V^{\infty}}{V^{rot}} \text{ (radial)}, \\ \dfrac{V^{rot}}{V^{\infty}}\dfrac{R^2}{r_A r} & \text{for } R\dfrac{V^{\infty}}{V^{rot}} < r \text{ (toroidal)}, \end{cases} \tag{4}$$

where R is the radius of the star, B^s its surface magnetic field, V^{rot} the surface rotation velocity, r_A the Alfvén radius which is given by the following equation

$$1 - R/r_A = \xi(R/r_A)^4 , \tag{5}$$

and

$$\xi = \frac{(B^s)^2 R^2}{2\dot{M} V^\infty} \simeq 0.07 \left(\frac{B^s}{10^2\ \mathrm{G}}\right)^2 \left(\frac{R}{20\ R_\odot}\right)^2 \times \left(\frac{\dot{M}}{2\times 10^{-5}\ M_\odot\ \mathrm{yr}^{-1}}\right)^{-1} \left(\frac{V^\infty}{2\times 10^3\ \mathrm{km\ s}^{-1}}\right)^{-1} . \quad (6)$$

From equation (5) the value r_A is

$$r_A \simeq R \times \begin{cases} (1+\xi) & \text{for } \xi \ll 1, \\ \xi^{1/4} & \text{for } \xi \gg 1 \end{cases} . \quad (7)$$

Upper limits of the surface magnetic field for the OB stars are a few hundred Gauss (Barker 1986). The value of B^s_{WR} for the WR stars may reach $\sim 10^4$ G (Mullan 1983; Nerney & Suess 1987; Maheswaran & Cassinelli 1988). The typical values of surface rotation velocity V^{rot} for the early-type stars are $V^{rot} \simeq (0.1\text{–}0.2)V^\infty$ (Conti & Ebbets 1977; Hutchings 1981; Uesugi & Fukuda 1982). The values of the Alfvén radius r_A for the early-type stars are in the range from $\sim R$ to $\sim(2\text{–}3)R$ (Usov & Melrose 1992).

To estimate the strength of magnetic field $B_{WR}(r)$ and $B_{OB}(r)$ in the WR and OB stellar winds it is necessary to substitute B^s_{WR}, $\dot{M}_{WR}$, R_{WR}, V^∞_{WR}, and V^{rot}_{WR} or B^s_{OB} $\dot{M}_{OB}$, R_{OB}, V^∞_{OB}, and V^{rot}_{OB} for B^s, $\dot{M}$, R, V^∞, and V^{rot}, respectively, in equations (4) and (6). Using these equations we can see that the strength of magnetic field near the shocks may be as high as $\sim$ a few ten G for close WR + OB binaries or $\sim$ a few G for wide WR + OB binaries.

2.4. *The Magnetic Field Direction near the Shock Fronts*

The value of $r_{WR} \simeq D$ for the WR + OB binaries is of the order of or more than $R_{WR}(V^\infty_{WR}/V^{rot}_{WR})$ if the rotation of the WR star is not anomalously slow, that is, $(V^{rot}_{WR} \gtrsim 0.1 V^\infty_{WR})$. Therefore, it is natural to expect that the toroidal component of the magnetic field near the shock S_1 is of the order or more than its poloidal component (see eq. [4] and Fig. 1). In this case the angle between the magnetic field $\boldsymbol{B}$ and unit vector $\boldsymbol{n}$ which is perpendicular to the shock front is more than $\pi/4$, that is the shock S_1 is quasi-perpendicular.

As to the magnetic field direction near the shock S_2 the situation is not so simple. A few versions may be the following:

1. If $r_{OB} < r_A$ the OB wind is suppressed by the ram pressure of the WR wind, on the side facing the WR star. In this case the WR wind collision with the magnetosphere of the OB star is similar to the collision of solar wind with the magnetospheres of planets (Hones 1979). Maybe this kind of wind interaction is realized in the very close binary V444 Cygni (WN4 + O6 binary with $P = 4.2$ days) for which the value of r_{OB} is equal to $\sim 1.2 R_{OB}$ (Usov 1990), and the collision region is very near the surface of the O star.

2. If $r_A < r_{OB} < R_{OB}(V^\infty_{OB}/V^{rot}_{OB})$ the magnetic field in the OB wind is radial near the collision region. The shock wave S_2 at the same point is quasi-parallel or quasi-perpendicular when the distance from the point to the line connecting the centers of the WR and OB stars is smaller or more than $\sim 2r_{OB}$ (Usov 1992a).

3. If $r_{OB} > R_{OB}(V^\infty_{OB}/V^{rot}_{OB})$, the toroidal component of the magnetic field dominates in all regions near the shock S_2, and the shock S_2 is quasi-perpendicular.

3. PARTICLE ACCELERATION AND NONTHERMAL RADIO EMISSION

It is well known that plasma shocks in an astrophysical setting can and do accelerate charged particles to high energies (see Blandford & Eichler 1987 and Ellison & Jones 1991 and references therein for reviews of shock acceleration theory). Therefore the strong shocks formed by the colliding stellar winds in massive binaries are very promising as particle accelerators.

Roughly the dynamical ram pressure ρV^2 ahead of both the shock S_1 and the shock S_2 is the same; here ρ and V are the mass density of the gas and its velocity ahead of the shock (Usov 1992a). Since $V^\infty_{WR} \sim V^\infty_{OB}$, we have $\rho_{WR} \sim \rho_{OB}$ near the shocks. Hence the parameters of both stellar winds ahead of the shocks are similar, and it is enough to discuss the particle acceleration by only one of the shocks. Let us consider necessary conditions for particle acceleration by the shock S_1. They include the following:

1. *The shock must be collisionless in the absence of an external injection mechanism.*—The postshock thermal collision time must be long compared to the ion gyroperiod. This is typically satisfied if the strength of the magnetic field ahead of the shock is

$$B \gg 10^{-6} \left(\frac{V^\infty_{WR}}{2\times 10^8\ \mathrm{cm\ s}^{-1}}\right)^{-3} \left(\frac{n}{10^{10}\ \mathrm{cm}^{-3}}\right) \mathrm{G} , \quad (8)$$

where

$$n \simeq \frac{\dot{M}_{WR}}{4\pi D^2 V^\infty_{WR} m_p \mu} \simeq 0.3\times 10^{10} \mu^{-1} \left(\frac{\dot{M}_{WR}}{2\times 10^{-5}\ M_\odot\ \mathrm{yr}^{-1}}\right) \times \left(\frac{D}{10^{13}\ \mathrm{cm}}\right)^{-2} \left(\frac{V^\infty_{WR}}{2\times 10^8\ \mathrm{cm\ s}^{-1}}\right)^{-1} \quad (9)$$

is the density of particles ahead of the shock, m_p is the proton mass, and μ is the mean molecular weight of the gas.

2. *The Ohmic damping rate of Alfvén waves must not exceed the maximum growth rate.*—This is more of an issue in dense winds than in, say, the interstellar medium or the solar wind. For primary acceleration of subrelativistic electrons this constraint can be shown to imply that

$$\frac{(V^\infty_{WR})^3}{V^2_{wh} V_{ph}} > 1.6\times 10^{-3} \left(\frac{n}{10^{10}\ \mathrm{cm}^{-3}}\right) \left(\frac{B}{\mathrm{G}}\right)^{-1} \epsilon^{-1} T_{eV}^{-3/2} \ln\Lambda . \quad (10)$$

Here V_{ph} is the phase velocity of the resonant waves, V_{wh} is the maximum whistler velocity, $[B^2/4\pi n m_e]^{1/2}$, $\ln\Lambda$ is the Coulomb logarithm, ϵ is the cosmic-ray partial pressure in units of the upstream ram pressure $\rho(V^\infty_{WR})^2$, and T_{eV} is the temperature of the gas ahead of the shock in eV.

In a wind from a massive star, the temperature is kept at about 1 eV by photoionization-recombination balance. The efficiency of shock acceleration ϵ for a single species has been calculated via a two-fluid approach, assuming ambient cosmic rays (Axford, Leer, & Skadron 1977), and by an explicit kinetic approach assuming the Alfvén wave scattering operates on thermal particles (Eichler 1979; Ellison & Eichler 1985). The results of the latter calculation are insensitive to the exact assumptions about injection as long as it saturates the acceleration mechanism. A feature of the cosmic-ray spectrum in the nonlinear theory is that the partial pressure in cosmic rays as a function of energy is slowly varying over the entire dynamic range of the cosmic rays, and if the phase velocity of the scatterers exceeds about 0.03 of the shock velocity, the partial pressure varies only by a factor of 3. The value of ϵ may be as high as several percent (Ellison & Eichler 1985).

The actual value of the phase velocity of the scatterers V_{ph}, however, is hard to determine. On the one hand, rapidly growing Alfvén waves can have highly super-Alfvénic velocities (Morrison et al. 1981; Fiorito, Eichler, & Ellison 1990). On the other hand, nonlinear scattering into the backward direction can counteract this effect, and even render the phase velocities of the Alfvén waves sub-Alfvénic. The observed spectra at the Earth's bow shock are consistent with sub-Alfvénic phase velocities (Ellison & Mobius 1987; D. C. Ellison 1992, private communication). In any case the value of V_{ph} cannot exceed the maximum value of whistler velocity V_{wh}. Taking this into account we have that equation (10) holds if

$$B < 2.7\left(\frac{V_{WR}^{\infty}}{2\times 10^{8}\ \mathrm{cm\ s^{-1}}}\right)^{3/2}\left(\frac{n}{10^{10}\ \mathrm{cm^{-3}}}\right)^{1/4}\left(\frac{\epsilon}{0.01}\right)^{1/2}\times\left(\frac{\ln\Lambda}{25}\right)^{-1/2} T_{eV}^{3/4}\ \mathrm{G}\ . \quad (11)$$

Here parameters V_{WR}^{∞}, n, ϵ, $\ln\Lambda$, and T_{eV} are normalized on their most reasonable values.

3. *For primary electron acceleration, the shock velocity must considerably exceed the phase velocity of whistler waves propagating normal to the shock, that is,* $V_{WR}^{\infty} \gg V_{ph}$.—Since $V_{ph} \lesssim V_{wh}$, condition 3 is met if $V_{WR}^{\infty} \gg V_{wh}$. The last condition may be written as

$$B \ll 2\left(\frac{V_{WR}^{\infty}}{2\times 10^{8}\ \mathrm{cm\ s^{-1}}}\right)\left(\frac{n}{10^{10}\ \mathrm{cm^{-3}}}\right)^{1/2}\mathrm{G}\ . \quad (12)$$

All of these constraints are typically satisfied by colliding winds in massive binaries. Hence the region of stellar wind collision in these binaries may be a strong source of both high-energy particles and nonthermal radiation generated by these particles.

The maximum electron energy is limited by ion-neutral wave damping and by inverse Compton losses (Bell 1978). The maximum energy, as limited by ion-neutral damping, is given by

$$E_{max} = 0.07\left(\frac{V_{WR}^{\infty}}{0.01c}\right)^{4/3}\left(\frac{n_e}{\mathrm{cm^{-3}}}\right)^{-1/3}\left(\frac{n_H}{\mathrm{cm^{-3}}}\right)^{-2/3}\left(\frac{f}{f_{gal}}\right)^{2/3}\mathrm{GeV}\ , \quad (13)$$

where n_e is the electron number density, n_H is the neutral hydrogen density, and f/f_{gal} is the ratio of cosmic-ray flux to that in the Galaxy. We take the latter ratio to be the cosmic-ray energy density in eV cm^{-3}. The total density in the pre-shock fluid is given by equation (9). The neutral hydrogen fraction is probably limited to of order 10^{-9} by the UV from the OB companion, and the neutral He fraction, He being about effective as neutral hydrogen for damping Alfvén waves, about 10^{-7}. Thus the neutral He and H, assuming cosmic abundances, contribute a number density of about $10^{2}(D/10^{13}$ cm$)^{-2}$ cm^{-3} where, as derived above, $n_e \sim 10^{9}(D/10^{13}$ cm$)^{-2}$ cm^{-3} (see eq. [9]). For efficient particle acceleration, the maximum energy allowed by ion neutral damping should be well above 100 GeV and does not play an important role.

Volk & Biermann (1988) have considered the possibility that the termination shocks in the winds of early-type stars accelerate ions all the way up to the highest Galactic cosmic-ray energies. We note that in their context, the field could be extremely wound up, and the cosmic rays might be trapped by the laminar field. Hence the high-energy cutoff quoted above may not apply there.

The limit for electrons on $E_{max} = \gamma_{max} m_e c^2$ due to inverse Compton losses can be shown, assuming a quasi-parallel shock geometry, to be given by

$$\gamma_{max}^2 < \frac{3\pi eBcr_{OB}^2}{\lambda\sigma_T L_{bol}}\left(\frac{V_{WR}^{\infty}}{c}\right)^2 \simeq 3\times 10^{8}\eta\left(\frac{V_{WR}^{\infty}}{2\times 10^{8}\ \mathrm{cm\ s^{-1}}}\right)^2\times\left(\frac{B}{\mathrm{G}}\right)\left(\frac{D}{10^{13}\ \mathrm{cm}}\right)^2\left(\frac{L_{bol}}{10^{39}\ \mathrm{ergs\ s^{-1}}}\right)^{-1}\ , \quad (14)$$

with approximate equality obtaining in the absence of any other, stronger limits. Here L_{bol} is the bolometric luminosity of the OB star, σ_T is the cross section of Thomson scattering, e is the electron charge, and $\lambda \simeq 3$ is the ratio of mean free path to gyroradius. This limit follows from the condition that the inverse Compton loss rate not exceed the acceleration rate, which is given by

$$\Gamma \simeq \left(\frac{V_{WR}^{\infty}}{c}\right)^2\frac{\Omega_{ce}}{\gamma_{max}\lambda}\ ,$$

where Ω_{ce} is the nonrelativistic electron cyclotron frequency. Note that since B varies as D^{-2} near the star, γ_{max} is insensitive to D for close binaries. When D is large enough that B varies as $1/D$, then γ_{max} should rise. However, if the field is wound up too tightly, it might quench the injection that is crucial to the creation of a cosmic-ray population. Given the constraints of B discussed above, the energy of electrons E_{max} can be shown to be enough to generate synchrotron radio emission at the frequencies of which nonthermal radio emission from massive binaries has been observed.

For a strong shock with the compression ratio of 4, the test particle theory predicts a spectrum of p^{-2} for accelerated particles (Krymsky 1977; Axford et al. 1977; Bell 1978; Blandford & Ostriker 1978). Efficient acceleration may, in principle, increase the shock compression ratio and may change the slope of the spectrum of accelerated particles, but nonlinear calculations yield a similar spectrum for a wide range of shock parameters (Ellison & Eichler 1985). In any case, the partial pressure in most ranges of relativistic electron energy is unlikely to be more than 0.05 of the total shock energy and could conceivably be much less (Blandford & Eichler 1987; Ellison & Reynolds 1991). Thus, for relativistic particles, the spectrum is similar to that obtained from the spectrum in the test particle theory for strong nonrelativistic shocks.

In this case a differential energy spectrum expected for relativistic electrons accelerated in the region of stellar wind collision is $N(E) \propto E^{-m}$, where $N(E)dE$ is the number of high-energy electrons per unit volume with total energy E in the interval dE and $m \simeq 2$. The spectrum of synchrotron radiation generated by relativistic electrons with this energy spectrum is $S(\nu) \propto \nu^{\alpha}$; here $S(\nu)$ is the flux of radiation at the frequency ν and $\alpha = -(m-1)/2 \simeq -0.5$ is a spectral index. It is worth noting that radio spectral indexes have been measured for about 200 supernova remnants for which the shock acceleration is the most probable mechanism of the high-energy particle's generation (Clark & Caswell 1976; Green 1984; see Reynolds 1988 for a review). It was shown that a mean value of α is near 0.5 with a relatively small spread. It is in good agreement with the frequency spectrum written above.

The expected value of nonthermal radio luminosity from the region of stellar wind collision is

$$L_{\rm rad} \simeq \epsilon\beta\zeta \frac{\dot{M}_{\rm WR}(V^{\infty}_{\rm WR})^2}{2}\left(\frac{\theta^2}{16}+0.22\eta\frac{V^{\infty}_{\rm OB}}{V^{\infty}_{\rm WR}}\right) \simeq 7.4\times10^{31}\beta \times\left(\frac{\epsilon}{10^{-2}}\right)\left(\frac{\zeta}{10^{-3}}\right)\left(\frac{\dot{M}_{\rm WR}}{2\times10^{-5}\,M_{\odot}\,{\rm yr}^{-1}}\right) \times\left(\frac{V^{\infty}_{\rm WR}}{2\times10^{8}\,{\rm cm\,s}^{-1}}\right)^2\left(\eta^{2/3}+0.8\eta\frac{V^{\infty}_{\rm OB}}{V^{\infty}_{\rm WR}}\right)\ {\rm ergs\ s}^{-1}, \quad (15)$$

where β is the ratio the energy density of high-energy electrons to the total energy density of cosmic rays ($0<\beta<1$), and

$$\zeta \simeq \frac{t_f}{t_s} \simeq 2\times10^{-5}\gamma\left(\frac{B}{\rm G}\right)^2\left(\frac{t_f}{10^4\ {\rm s}}\right) \simeq 4\times10^{-3}\eta^{1/2}\left(\frac{B}{\rm G}\right)^{3/2} \times\left(\frac{D}{10^{13}\ {\rm cm}}\right)\left(\frac{V^{\infty}_{\rm WR}}{2\times10^{8}\ {\rm cm\ s}^{-1}}\right)^{-1}\left(\frac{\nu}{5\ {\rm GHz}}\right)^{1/2} \quad (16)$$

is the fraction of the energy in high-energy electrons that is lost to synchrotron radiation, $t_s \simeq 5\times10^{8}\gamma^{-1}(B/{\rm G})^{-2}$ s is the characteristic time of energy loss by a relativistic electron with the Lorentz factor γ via the synchrotron radiation,

$$t_f \simeq \frac{r_{\rm OB}}{V^{\infty}_{\rm WR}} \simeq 0.5\times10^{5}\eta^{1/2}\left(\frac{D}{10^{13}\ {\rm cm}}\right)\left(\frac{V^{\infty}_{\rm WR}}{2\times10^{8}\ {\rm cm\ s}^{-1}}\right)^{-1}{\rm s} \quad (17)$$

is the flow time in the colliding wind region, and ν is the frequency of radio observations. The value of the dimensionless parameter β may be estimated from spectrum observations of γ-ray emission generated in the region of stellar wind collision (see § 5).

To get equation (16) it is taken into account that the Lorentz factor of electrons generating synchrotron radio emission at the frequency $\sim\nu$ is

$$\gamma \simeq 40\left(\frac{B}{\rm G}\right)^{-1/2}\left(\frac{\nu}{5\ {\rm GHz}}\right)^{1/2}. \quad (18)$$

First and second terms of the sum in brackets of equation (15) are some geometrical factors of the stellar wind collision (Usov 1992a) and correspond to the synchrotron radio emission of high-energy electrons accelerated by the shocks S_1 and S_2, respectively.

Typically, only a small fraction of the cosmic-ray energy can be converted to radio emission before the flow convects them out of the colliding wind region.

From equation (2) we can get the characteristic size of nonthermal radio emission

$$l^{\rm rad} \simeq 2R_c(\pi/2) \simeq \pi r_{\rm OB}. \quad (19)$$

4. RADIO STRUCTURE AND RADIO VARIABILITY

Stellar winds outflowing from the WR and OB stars are opaque to free-free absorption. The radius of optical depth unity to free-free absorption, that is, the radius of the radio photosphere at the frequency ν is (Wright & Barlow 1975)

$$R^{\rm rad} \simeq 2.2\times10^{14}\left(\frac{\dot{M}}{2\times10^{-5}\,M_{\odot}\,{\rm yr}^{-1}}\right)^{2/3}\left(\frac{V^{\infty}}{2\times10^{3}\ {\rm km\ s}^{-1}}\right)^{-2/3} \times\left(\frac{T}{10^4\ {\rm K}}\right)^{-1/2}\left(\frac{\nu}{5\ {\rm GHz}}\right)^{-2/3}{\rm cm}. \quad (20)$$

A typical radius of the radio photosphere at the frequency of a few GHz for WR stars is $R^{\rm rad}_{\rm WR} \simeq$ a few times 10^{14} cm. The value of this radius for OB stars, $R^{\rm rad}_{\rm OB}$, is approximately an order of magnitude smaller than $R^{\rm rad}_{\rm WR}$. Hence, in the case of early-type stars the radius of their radio photosphere is of the order of a hundred or more stellar radii.

In the previous section it was shown that the region of stellar wind collision may be a strong source of nonthermal radio emission. The radius of this source is $\sim 1.5r_{\rm OB} \ll D$. The observational properties of nonthermal radio emission depend substantially on the ratio $\xi_1 = R^{\rm rad}_{\rm WR}/r_{\rm WR} \simeq R^{\rm rad}_{\rm WR}/D$.

Let us consider the structure of nonthermal radio sources and radio variability for WR + OB binaries with nearly circular orbits. If the binary is wide and $\xi_1 < 1$ (orbital period $P \gtrsim 10$ yr) the region of stellar wind collision, where the nonthermal radio emission is mainly generated, is outside the radio photosphere of the WR star. If the angle φ between the line of sight and the orbital plane is small enough ($\varphi \lesssim \xi_1$, here the angle φ is in radius), the flux of nonthermal radio emission will be modulated because of the eclipse of the region of stellar wind collision by the stellar winds. When $\varphi > \xi_1$ the flux of nonthermal radio emission practically does not vary if the gas outflow from the WR and OB stars is stationary.

The expected time variations of nonthermal radio emission are very slow irrespective of the ratio φ/ξ_1 if the value of ξ_1 is more than a few times smaller than unity. It is because $P \gg 10$ yr in this case. The radio-bright WR star AS 431 is probably the radio source of this kind. There is an indication that this star is the binary of which the orbital period is a few thousand years (Moran et al. 1989). Therefore, the observational fact that the nonthermal radio emission of AS 431 does not vary is natural. As expected in the model of generation of nonthermal radio emission in the region of stellar wind collision, the source of nonthermal radio emission of AS 431 is near the component of the WR star. The observed values of $\xi_1 \simeq 0.3$ and $r_{\rm OB}/D \simeq \frac{1}{6}$ for binary AS 431 (Moran et al. 1989) are in good agreement with the values expected for stellar wind collision (regarding the generation of radio and X-ray emission in AS 431, see Usov 1992b).

If $\xi_1 > 1$ the source of nonthermal radio emission which coincides with the region of stellar wind collision is inside the radius of the radio photosphere for the WR star. This source may be observed at the frequency ν only if the time $R^{\rm rad}_{\rm WR}/V^{\infty}_{\rm WR}$ during which the gas outflowing from the WR star with the velocity $V^{\infty}_{\rm WR}$ reaches the radius of the radio photosphere $R^{\rm rad}_{\rm WR}$ is of the order of or smaller than the time which is necessary for the WR + OB binary to turn on the angle $2\theta + \Delta\theta \simeq 3\theta$ (see Fig. 1), that is,

$$\frac{R^{\rm rad}_{\rm WR}}{V^{\infty}_{\rm WR}} \lesssim \frac{3\theta}{2\pi}P \quad (21)$$

or $P \gtrsim P_{\rm cr}$, where

$$P_{\rm cr} = \frac{2\pi}{3\theta}\frac{R^{\rm rad}_{\rm WR}}{V^{\infty}_{\rm WR}} \simeq 13\left(1-\frac{\eta^{2/5}}{4}\right)^{-1}\eta^{-1/3} \times\left(\frac{\dot{M}_{\rm WR}}{2\times10^{-5}\,M_{\odot}\,{\rm yr}^{-1}}\right)^{2/3}\left(\frac{V^{\infty}_{\rm WR}}{2\times10^{3}\ {\rm km\ s}^{-1}}\right)^{-5/3} \times\left(\frac{T}{10^4\ {\rm K}}\right)^{-1/2}\left(\frac{\nu}{5\ {\rm GHz}}\right)^{-2/3}{\rm days}. \quad (22)$$

For a typical WR + OB binary ($\dot{M}_{\rm WR} \simeq 2\times10^{-5}\,M_{\odot}\,{\rm yr}^{-1}$, $V^{\infty}_{\rm WR} \simeq 2\times10^{3}$ km s^{-1}, $\eta \simeq 0.1$, $T \simeq 10^4$ K at $r \simeq R^{\rm rad}_{\rm WR}$) the

value of P_{cr} is of the order of a month when the frequency of observation is a few GHz.

If $P < P_{cr}$ nonthermal radio emission from the region of stellar wind collision in the WR + OB binary cannot be observed because it is screened by the WR wind.

In the case of $P \gtrsim P_{cr}$ nonthermal radio emission from the WR + OB binary may be detected if the angle φ is smaller $3\theta/2$. In this case the character of expected radio variability depends on the ratio R_{OB}^{rad}/r_{OB}. If $R_{OB}^{rad} < r_{OB}$ the flux of nonthermal radio emission varies slightly when the observer is inside the conic surface $\tilde{C}$. If R_{OB}^{rad} is more than a few r_{OB}, nonthermal radio emission escaping from the region of stellar wind collision is concentrated near the conic surface $\tilde{C}$. Therefore, if the angle φ is smaller than the angle θ, the observer will detect two radio bursts corresponding to the two configurations in which the conic surface $\tilde{C}$ intersects the sight of light. The time interval between the radio bursts is

$$\Delta t_0 \simeq \frac{1}{\pi} \arccos\left(\frac{\cos\theta}{\cos\varphi}\right) P . \tag{23}$$

The duration of radio bursts Δt_1 depends on many factors, such as the values of θ and φ, structure of the region of nonthermal radiation, additional screening of the radio-radiating region by the curved stream of outflowing gas at the distance $r \sim R_{WR}^{rad}$, etc. It is possible both $\Delta t_1 \ll \Delta t_0$ and $\Delta t_1 \sim \Delta t_0$.

If the orbital eccentricity of the WR + OB binary is large, the ratios R_{WR}^{rad}/r_{WR} and R_{OB}^{rad}/r_{OB} vary, and the WR + OB binary moves from one kind of nonthermal radio source to another in the process of orbital motion.

5. WR 140: INTERPRETATION OF SOME OBSERVATIONAL DATA AND THEORETICAL PREDICTIONS

Anomalously strong infrared, X-ray, and radio emission was observed from WR 140 (see Williams et al. 1990 for a summary of observed properties). Most probably, the stellar wind collision is responsible for the additional radiation of WR 140 in all three regions (Williams et al. 1987; Pollock 1987; Williams et al. 1990; Usov 1991, 1992a).

5.1. *Main Parameters of WR 140*

WR 140 is a binary system composed of a WC 7 and an O4-5. The orbital parameters of WR 140 and the parameters of the stellar winds outflowing from its components are the following: the orbital period $P = 2900 \pm 10$ d (7.94 yr), the semimajor axis $a = 14.7$ AU, the eccentricity $e = 0.84 \pm 0.04$, $\omega = 32° \pm 8°$, $D_{min} = (1 - e)a \simeq 3.5 \times 10^{13}$ cm, $D_{max} = (1 + e)a \simeq 4 \times 10^{14}$ cm, $\dot{M}_{WR} \simeq 5.7 \times 10^{-5}\ M_\odot\ \mathrm{yr}^{-1}$, $V_{WR}^{\infty} \simeq 2860$ km s^{-1}, $\dot{M}_{OB} \simeq 1.6 \times 10^{-6}\ M_\odot\ \mathrm{yr}^{-1}$, and $V_{OB}^{\infty} \simeq 3200$ km s^{-1} (Conti 1988; Williams & Eenens 1989; Williams et al. 1990). The mass of the O4-5 star equals $\sim 38\ M_\odot$, that is, ~ 3 times more than the mass of the WC 7 star.

Substituting these parameters into equations (1)–(3), (20), and (22), we obtain $\eta = 0.031$, $r_{WR} \simeq 0.85D$, $r_{OB} \simeq 0.15D$, $\theta \simeq 0.63$ rad $\simeq 36°$, $R_{WR}^{rad} \simeq 3.5 \times 10^{14}$ cm, $R_{OB}^{rad} \simeq 2 \times 10^{13}$ cm, and $P_{cr} \simeq 4 \times 10^6$ s $\simeq 48$ days. The values of R_{WR}^{rad}, R_{OB}^{rad}, and P_{cr} are evaluated at the frequency $\nu = 5$ GHz for $T = 10^4$ K at $r \simeq R_{WR}^{rad}$.

5.2. *Variations of Radio Emission*

Striking variations of radio emission from WR 140 were observed. It was shown that WR 140 may be in a "radio low" or "radio high" state (Florkowski & Gottesman 1977; Florkowski 1982; Becker & White 1985; Abbott et al. 1986). In the radio low state the flux of radio emission at the frequency 5 GHz is $S_{th}(5\ \mathrm{GHz}) \simeq 1.5$ mJy. This steady radio emission has a spectral index α with the canonical 0.6 value for a thermal wind and comes from the ionized wind of WR 140.

The observations of radio emission from WR 140 are very rare. Therefore, until now the data on the transition of WR 140 from its radio low state to radio high state and back were very poor. We can see only that the additional radio emission has appeared at the orbital phase $\phi \simeq 0.3$ (Williams et al. 1990). At first this radio emission increases slowly. The transition from the low state to the high state is somewhere at $\phi \simeq 0.5$–0.6 (see Fig. 2). Additional radio emission reaches a maximum $S_{nth}(5\ \mathrm{GHz}) \gtrsim 24$ mJy at $\phi \simeq 0.8$ and then very rapidly declines at $\phi \simeq 0.9$. The 2–6 cm spectral index of additional radio emission α changes dramatically, from $\alpha \simeq -0.5$ near maximum to $\alpha = 1.7$ as the radio source disappears, arguing for a nonthermal nature of additional radio emission. Let us try to explain the behavior of the additional radio emission of WR 140 under the supposition that this radio emission is generated in the region of stellar wind collision.

Most probably, the time variability observed for nonthermal radio emission of WR 140 is a result of both the variation of the distance between the components of the WC 7 + O4-5 binary in the process of orbital rotation and the absorption of radio emission in the stellar winds. At the orbital phase $\phi \simeq 0.3$ the value of r_{WR} is 3.1×10^{14} cm, which is close to the value of $R_{WR}^{rad} \simeq 3.5 \times 10^{14}$ cm, and nonthermal radio emission of WR 140 appears for the observer. The optical depth τ for nonthermal radio emission at $\phi \simeq 0.3$ may be estimated as

$$\tau \simeq 2\left(\frac{R_{WR}^{rad}}{r_{WR}}\right)^3 \frac{\delta - \sin\delta\cos\delta}{\sin^3\delta} \simeq 2.8 , \tag{24}$$

where $\delta = \sigma - \psi \simeq 70°$ is the angle between the sightline and the line connecting the components of the binary at $\phi \simeq 0.3$, $\sigma = \pi/2 - \omega = 58° \pm 8°$, and $\psi \simeq -12°$ is the angle between the line connecting the components and the main axis of the binary (see Fig. 3 at which the angle ψ is zero at $\phi = 0.5$, $\psi < 0$ at $0 \le \phi < 0.5$, and $\psi > 0$ at $0.5 < \phi \le 1$). Here and below we assume that the inclination of orbit $i = \pi/2 - \varphi$, that is, the angle between the sight line and the normal to the orbit, is near $\pi/2$.

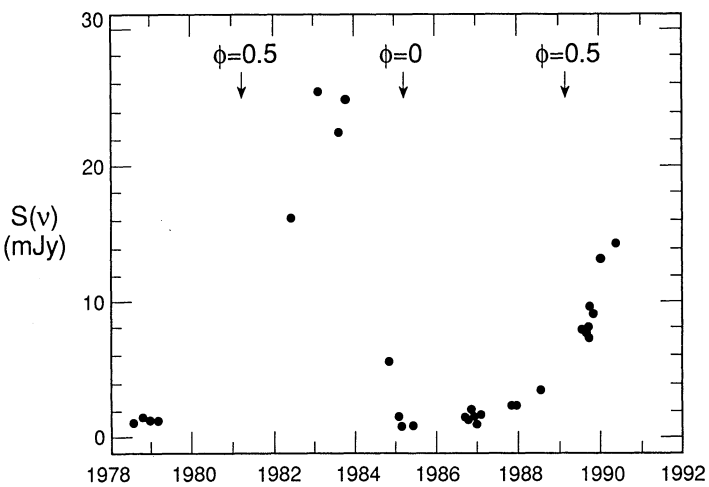

FIG. 2.—Radio light curve of WR 140 at the frequency $\nu = 5$ GHz. The orbital phase ϕ is shown by the arrows.

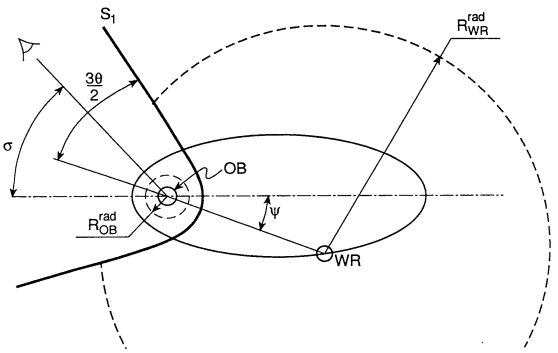

FIG. 3.—Schematic structure of WR 140 at the orbital phase $\phi \simeq 0.7$. σ is the angle between the sightline and the main axis of the binary. R_{WR}^{rad} and R_{OB}^{rad} are the radii of the radio photosphere for the WR and OB stars, respectively.

The detected flux of nonthermal radio emission $S_{nth}(5\ \mathrm{GHz}) \simeq S_{th}(5\ \mathrm{GHz}) \simeq 1.5$ mJy at $\phi \simeq 0.3$ is $\sim e^{\tau} \simeq 16$ times smaller than the intrinsic intensity without any absorption of radio emission in the WR wind. This is in good agreement with the flux of nonthermal radio emission $S_{nth}(5\ \mathrm{GHz}) \simeq 24$ mJy observed at $\phi \simeq 0.73$ when the value of D was practically the same as at $\phi \simeq 0.3$ and when the absorption of radio emission was very small (see below).

In the phase interval from $\phi \simeq 0.3$ to $\phi \simeq 0.5$–0.6 the flux of nonthermal radio emission increases slowly due to the slow decrease of the optical depth. In this interval of ϕ the behavior of nonthermal radio emission was described by Williams et al. (1990).

At $\phi \simeq 0.5$–0.6 we have $\psi + 3\theta/2 \simeq \sigma$, and the observer intersects the conic surface $\tilde{S}_1$ (see Fig. 3). The characteristic time of orbital motion at this moment is a few times more than the value of P_{cr} at the frequency $\nu \gtrsim$ a few GHz. In this case the twist of the surface S_1 at the distance $r \simeq R_{WR}^{rad}$ is small, that is, the surface S_1 practically coincides with the conic surface $\tilde{S}_1$ at $r_{OB} \ll r \lesssim R_{WR}^{rad}$. The absorption of nonthermal radio emission in the WC 7 wind is absent when the observer is inside this conic surface. Besides, the size of nonthermal radio source is $l^{rad} \simeq \pi r_{OB} \simeq 0.47D \simeq 1.8 \times 10^{14}$ cm (see § 3). That is essentially more than the diameter of radio photosphere $2R_{OB}^{rad} \simeq 0.4 \times 10^{14}$ cm for the O4-5 star at the frequency $\nu = 5$ GHz. Therefore, leading off the orbital phase $\phi \simeq 0.5$–0.6 the main part of nonthermal radio emission generated in the region of stellar wind collision at the frequency $\nu \gtrsim$ a few GHz is observed practically without absorption. *From this moment WR 140 is in the radio high state.*

At the frequency $\nu <$ (1–2) GHz the twist of the surface S_1 at the distance $r \simeq R_{WR}^{rad}$ becomes essential for the observation of the nonthermal radio source. The result of this is that the transition from the radio low state to the radio high state at low frequencies has to be later than at high frequencies.

The value of r_{OB} decreases in the process of subsequent orbital motion at $\phi > 0.5$, and hence the size of nonthermal radio source decreases as well. When the phase ϕ is ~ 0.93, the value of r_{OB} is equal to R_{OB}^{rad} at the frequency $\nu = 5$ GHz. Therefore, at $\phi \gtrsim 0.9$ the flux of nonthermal radio emission at $\nu = 5$ GHz decreases due to the eclipse of the region of stellar wind collision by the stellar wind of the O4-5 star. From the moment when ϕ is ~ 0.9 WR 140 turns into the radio low state at the frequency 5 GHz.

Since the value of R_{OB}^{rad} at the frequency $\nu = 15$ GHz is 2.1 times smaller than at the frequency $\nu = 5$ GHz, the strong nonthermal radio emission at $\nu = 15$ GHz was observed until 1984.80 ($\phi \simeq 0.94$). The value of r_{OB} is equal to R_{OB}^{rad} at $\nu = 15$ GHz when $\phi \simeq 0.97$. The drop of nonthermal radio emission at the frequency $\nu = 15$ GHz is expected somewhere at $\phi \simeq 0.95$–0.96.

A very interesting phenomenon may be observed at $\phi = 0.98 \pm 0.005$, namely, at this orbital phase the observer is near the conic surface $\tilde{C}$ again, and a strong radio burst may be observed at high enough frequencies. The expected duration of this radio burst is two or three weeks. Near periastron the characteristic time of orbital motion is of the order of P_{cr} at the frequency of a few GHz (see eq. [10]). Therefore, the low boundary of the frequency of the radio burst is determined by the absorption of radio emission in the outflowing gas of which the stream lines are twisted due to orbital rotation (see § 4).

Beginning from $\phi \simeq 0.99$ nonthermal radio emission cannot be observed from WR 140 at any frequency since the region of stellar wind collision is screened by the radio photosphere of the WC 7 star. The flux of total radio emission of WR 140 has to be minimum at $\phi \simeq 0.008$ when the O4-5 star is behind the WC 7 star (see Fig. 3). At this moment only the thermal radio emission of the WC 7 wind undisturbed by the stellar wind collision is observed. The duration of this minimum is a few months. At $\phi \simeq 0.05 \pm 0.01$ the flux of thermal radio emission of WR 140 has to be several tens of percent more than at $\phi \simeq 0.008$ due to the compression of the part of the outflowing gas in the shock layers (Usov 1992a).

5.3. *Radio Luminosity and Radio Spectrum*

Substituting the parameters of WR 140 into equation (15) we obtain the following equation for the expected nonthermal radio luminosity from the region of stellar wind collision

$$L^{rad} \simeq 5.4 \times 10^{31} \beta \left(\frac{\epsilon}{0.01}\right)\left(\frac{\zeta}{10^{-3}}\right) \mathrm{ergs\ s^{-1}}\ . \qquad (25)$$

For reasonable values $\beta \sim 0.1$ and $\epsilon \sim 0.01$, this luminosity coincides with the observed value $L_{5\,GHz}^{rad} \simeq 5 \times 10^{29}$ ergs s^{-1} at 5 GHz at the radio high state ($\phi \simeq 0.7$) if $\zeta \sim 10^{-4}$. From equation (16) we can estimate the strength of the magnetic field in the region of stellar wind collision at the orbital phase $\phi = 0.7$ ($D \simeq 3.6 \times 10^{14}$ cm) as $B \simeq 0.03$ G. This magnetic field meets necessary conditions for particle acceleration by the shocks (see § 3). The surface magnetic field of the components of WR 140 obtained by the extrapolation from the region of stellar wind collision to the surface of the stars by the use of equations (4)–(7) is near the upper bounds existing for these kinds of massive stars as is assumed by Usov & Melrose (1992) to explain the X-ray emission of single massive stars.

Using equations (16) and (25) it is possible to get a lower bound for the strength of the magnetic field in the region of stellar wind collision. Indeed, from conditions $L^{rad} = L_{5\,GHz}^{rad} \simeq 5 \times 10^{29}$ ergs s^{-1}, $\beta < 1$, $\epsilon \lesssim 0.05$, and equations (16) and (25), we can get $\zeta \gtrsim 2 \times 10^{-6}$ and $B \gtrsim 10^{-3}$ G. Hence, the strength of the magnetic field ahead of one of the shocks or ahead of both shocks at $\phi \simeq 0.7$ has to be in the range from ~ 0.1 to $\sim 10^{-3}$ G with the most probable value $B \sim 10^{-2}$ G, that is, $2 \times 10^{-6} \lesssim \zeta \lesssim 10^{-3}$. The upper bound for the B-value follows from necessary conditions for shock acceleration.

The spectral index $\alpha = -0.5$ predicted by the theory of particle acceleration by a strong shock (see § 3) is in agreement with the value of α observed at the radio high state when the absorption of radio emission is small. Most probably, the change in spectral index observed at the moment of the tran-

sition of WR 140 from its radio high state to radio low state is connected with the absorption of low-frequency radio emission in the gas of the stellar winds (Williams et al. 1990). A study of the spectral index variations are beyond the framework of this paper and will be addressed elsewhere.

5.4. *The Size of Nonthermal Radio Emission*

The visible size of the nonthermal radio source in the radio high state is

$$l_{\perp}^{\rm rad} \simeq l^{\rm rad} \cos(\sigma - \psi) \simeq \pi r_{\rm OB} \cos(\sigma - \psi) . \quad (26)$$

The projected separation of the binary components is

$$D_{\perp} = D \sin(\sigma - \psi) . \quad (27)$$

From (1), (26), and (27) we have

$$\frac{l_{\perp}^{\rm rad}}{D_{\perp}} \simeq \pi \frac{\eta^{1/2}}{1 + \eta^{1/2}} \tan^{-1}(\sigma - \psi) . \quad (28)$$

Recently the radio source associated with WR 140 was observed at $\nu = 5$ GHz with the European VLBI Network plus the VLA at $\phi = 0.62$ ($\psi \simeq 8°$) by Felli & Massi (1991). Using $\sigma = 58° \pm 8°$ we can see that the value of the ratio $l_{\perp}^{\rm rad}/D_{\perp}$ expected at the time of the observations is in the interval between 0.3 and 0.52. This is in agreement with the observed value $l_{\perp}^{\rm rad}/D_{\perp} = 0.45 \pm 0.03$ (Felli & Massi 1991).

5.5. *Gamma-Ray Emission*

Gamma-ray emission can be attributed to either inverse Compton emission or p-p collisions followed by pion decay. In the former case, the seed photons would presumably be the processed UV radiation from the O4-5 star. Inverse Compton spectrum of γ-rays has an exponential high-energy cutoff at the energy

$$E_{\rm max} \simeq (4/3) E_{\rm UV} \gamma_{\rm max}^2 \simeq 4 \times 10^9 \eta \left(\frac{V_{\rm WR}^{\infty}}{2 \times 10^8 \text{ cm s}^{-1}}\right)^2 \left(\frac{B}{\rm G}\right) \times \left(\frac{D}{10^{13} \text{ cm}}\right)^2 \left(\frac{L_{\rm bol}}{10^{39} \text{ ergs s}^{-1}}\right)^{-1} \text{eV} , \quad (29)$$

where $E_{\rm UV} \simeq 10$ eV is the mean energy of UV photons radiated by the O4-5 star of which the effective temperature is $\sim$44,000 K (Williams et al. 1990). Using $L_{\rm bol} \simeq 1.7 \times 10^{39}$ ergs s^{-1}, $B \simeq 0.01$ G, $\eta \simeq 0.031$, and $D \simeq 3.6 \times 10^{14}$ cm, we have $E_{\rm max} \simeq 10^3$ MeV at $\phi \simeq 0.7$.

For high-energy electrons with $\gamma \sim \gamma_{\rm max}$ the characteristic time of energy loss via the inverse Compton radiation is smaller than the flow time t_f given by equation (17). Therefore, the main fraction of energy of relativistic electrons with $\gamma \sim \gamma_{\rm max}$ is radiated and transfers into γ-rays before the flow convects these electrons out of the colliding wind region. In this case the expected value of γ-ray luminosity of WR 140 L_{γ} is of the order of the luminosity of the shocks L_e in the high-energy electrons. From determination of ζ it is followed that $L_e = \zeta^{-1} L^{\rm rad}$ (see § 3). Hence, we have

$$L_{\gamma} \sim L_e = \zeta^{-1} L^{\rm rad} \simeq 5 \times 10^{32}\text{–}2.5 \times 10^{35} \text{ ergs s}^{-1} , \quad (30)$$

where $2 \times 10^{-6} \lesssim \zeta \lesssim 10^{-3}$.

The maximum value of L_{γ} is enough to explain the γ-ray flux observed with *COS B* from the γ-ray source 083+03 which is near WR 140 (Pollock et al. 1985). At the moment of γ-ray observation WR 140 was near the periastron passage when the physical conditions in this binary is the most favorable for γ-ray generation. Therefore future γ-ray observations with *EGRET* at the next periastron passage in 1993.2 are very promising. They can help to estimate the value of the magnetic field near the shocks more precisely than above.

Finally, we note that both γ-rays and relativistic electrons can be generated via the decay of pions that emerge from p-p collisions. In a typical convection time t_f, relativistic protons pass through $\sim n t_f c \sim 10^{23}$–$10^{24}$ protons cm^{-2}, so conversion efficiencies of order 10% are plausible. Hence, neither the radio nor the γ-ray emission yet prove the existence of primary electron acceleration in WR 140. However, there should be no high-energy spectral cutoff for pion decay γ-rays, only a lower one corresponding to the pion production threshold. Therefore it is possible to separate the inverse Compton γ-ray emission and γ-rays generated by pion decay and to estimate the value of β. Moreover, the pionization conversion efficiency should be proportional to D^{-1}, unlike the inverse Compton luminosity.

6. SUMMARY AND DISCUSSION

We have considered in this paper the generation of nonthermal radio emission in binaries of early-type stars like WR + OB binaries. It is shown that the region of stellar wind collision in these binaries may be a strong source of nonthermal radio and γ-ray emission. Nonthermal radio emission may be observed only if the orbital period of a binary is more than some critical value $P_{\rm cr}$. The value of $P_{\rm cr}$ depends on the frequency at which nonthermal radio emission is observed. For WR + OB binaries, for example, the values of $P_{\rm cr}$ cover a range from a month to a few months when the frequency of radio observations is 5 GHz.

Basic observational data on the nonthermal radio emission of WR 140, such as luminosity, spectrum, time variability in the process of orbital motion, the size of nonthermal radio source, etc., are explained in the framework of a model in which nonthermal radio emission is generated in the region of stellar wind collision. Since the motion of outflowing gas and its parameters vary in the region of stellar wind collision (see Fig. 1), it is possible to observe nonthermal radio emission of WR 140 generated deep inside the radius photospheres of the WC 7 wind.

Given the nonthermal radio emission observation from the region of stellar wind collision in WR 140, it follows that the inclination of the orbit is $i > \pi/2 - 3\theta/2 \simeq 36°$. From the condition that the observer is near the conic surface $\tilde{S}_1$ when the orbital phase is $\phi \simeq 0.5$–0.6 ($\psi \simeq 0°$–$6°$) we can get the following estimate: $60° \lesssim i \lesssim 90°$. To define the i-value more precisely it is necessary to do both detailed multifrequency observations of the transition of WR 140 from the radio low state to the radio high state and back as well as precise calculations of the form of the shock waves far from the binary.

The next periastron passage of WR 140 is in 1993.2. The drop of nonthermal radio emission at the frequency of a few GHz is expected at the orbital phase $\phi \simeq 0.9$. Most probably, the drop is due to the eclipse of the wind collision site by the stellar wind of the O4-5 star. The radio photosphere of the O4-5 star is like a screen whose radius depends on the frequency of the detected radio emission. To investigate the structure of nonthermal radio source the multifrequency observations of the eclipse are necessary. Detection of synchrotron emission at two different orbital configurations would provide information about the magnetic field in the winds.

The radio emission already observed from WR 140 together with the optical and UV luminosity of the O4-5 star and likely parameters for the magnetic field suggest an inverse Compton luminosity up to a few 10^{35} ergs s^{-1} at tens to hundreds of MeV, consistent with an identification with the *COS B* source. *EGRET* observations may be able both to identify a high-energy cutoff in the inverse Compton spectrum, corresponding to the energy where the loss time equals the shock acceleration time, and to separate the inverse Compton γ-ray emission and γ-rays generated by pion decay. Prolonged observation by *EGRET* may also detect time dependence in the γ-ray emission, which is expected if the γ-radiation comes from p-p collisions.

We are grateful to Professor M. Milgrom for helpful conversations. This research was supported in part by the Israel-US Binational Science Foundation and Einstein Centre for Theoretical Physics.

REFERENCES

Abbott, D. C., Bieging, J. H., Churchwell, E., & Torres. A. V. 1986, ApJ, 303, 239
Abbott, D. C., & Conti, P. S. 1987, ARA&A, 25, 113
Axford, W. I., Leer, E., & Skadron, A. 1977, in Proc. 15th Internat. Cosmic Ray Conf. (Plovdiv), 11, 32
Barker, P. K. 1986, PASP, 98, 44
Becker, R. H., & White, R. L. 1985, ApJ, 297, 649
Bell, A. R. 1978, MNRAS, 182, 147
Bieging, J. H., Abbott, D. C., & Churchwell, E. B. 1989, ApJ, 340, 518
Blandford, R. D., & Eichler, D. 1987, Phys. Rep., 154, 1
Blandford, R. D., & Ostriker, J. P. 1978, ApJ, 227, L49
Chen, W., & White, R. L. 1991, ApJ, 366, 512
Chlebowski, T. 1989, ApJ, 342, 1091
Chlebowski, T., Harnden, F. R., Jr., & Sciortino, S. 1989, ApJ, 341, 427
Clark, D. H., & Caswell, F. L. 1976, MNRAS, 174, 257
Conti, P. S. 1978, ARA&A, 16, 371
———. 1988, in O Stars and Wolf-Rayet Stars, ed. P. S. Conti & A. B. Underhill (NASA SP-497), 121
Conti, P. S., & Ebbets, D. 1977, ApJ, 213, 438
Dickel, H. R., Habing, H. J., & Isaacsman, R. 1980, ApJ, 238, 439
Eichler, D. 1979, ApJ, 229, 419
Ellison, D. C., & Eichler, D. 1985, Phys. Rev. Lett., 55, 2735
Ellison, D. C., & Jones, F. C. 1991, Space Sci. Rev., 58, 259
Ellison, D. C., & Mobius, E. 1987, ApJ, 318, 474
Ellison, D. C., & Reynolds, S. P. 1991, ApJ, 382, 241
Felli, M., & Massi, M. 1991, A&A, 246, 503
Felli, M., & Panagia, N. 1982, ApJ, 262, 650
Fiorito, R. B., Eichler, D., & Ellison, D. C. 1990, ApJ, 364, 582
Florkowski, D. R. 1982, in IAU Symp. 99, Wolf-Rayet Stars: Observations, Physics, Evolution, ed. C. W. H. de Loore & A. J. Willis (Dordrecht: Reidel), 63
Florkowski, D. R., & Gottesman, S. T. 1977, MNRAS, 179, 105
Garmany, C. D., & Conti, P. S. 1984, ApJ, 284, 705
Girard, T., & Willson, L. A. 1987, A&A, 183, 247
Green, D. A. 1984, MNRAS, 209, 44
Hogg, D. E. 1982, in IAU Symp. 99, Wolf-Rayet Stars: Observations, Physics, and Evolution, ed. C. W. H. de Loore & A. J. Willis (Dordrecht: Reidel), 221
———. 1985, in Radio Stars, ed. R. Hjellming & G. Gibson (Dordrecht: Reidel), 117
Hones, E. W., Jr. 1979, Space Sci. Rev., 23, 393
Hutchings, J. B. 1981, PASP, 93, 50
Krymsky, G. F. 1977, Dokl. Akad. Nauk. SSR, 234, 1306
Lebedev, M. G., & Myasnikov, A. V. 1988, in Numerical Methods in Aerodynamics, ed. V. M. Paskonov & G. S. Poslyakov (Moscow: Moscow State University), 3
Leitherer, C. 1988, ApJ, 236, 356
Luo, D., McCray, R., & Mac Low, M.-M. 1990, ApJ, 362, 267
Maheswaran, M., & Cassinelli, L. P. 1988, ApJ, 335, 931
Moffat, A. F. J., Firmani, C., McLlean, L. S., & Seggewiss, W. 1982, in IAU Symp. 99, Wolf-Rayet Stars: Observations, Physics, Evolution, ed. C. W. H. de Loore & A. J. Willis (Dordrecht: Reidel), 577
Moran, J. P., Davis, R. J., Bode, M. F., Taylor, A. R., Spencer, R. E., Argue, A. N., Irwin, M. J., & Shanklin, J. D. 1989, Nature, 340, 449
Morrison, P. J., Scott, J. Holman, G. D., & Ionson, J. A. 1981, preprint
Mullan, D. J. 1983, Irish Astron. J., 16, 107
Nerney, S., & Suess, S. T. 1987, ApJ, 321, 355
Panagia, N., & Felli, M. 1975, A&A, 39, 1
Pollock, A. M. T. 1987, ApJ, 320, 283
Pollock, A. M. T., et al. 1985, A&A, 146, 352
Prilutskii, O. F., & Usov, V. V. 1975, Astron. Tsirk., 854, 1
———. 1976, Soviet Astron., 20, 2
Reynolds, S. P. 1988, in Galactic and Extragalactic Radio Astronomy, ed. G. L. Verschuur & K. I. Kellermann (New York: Springer), 439
Stevens, I. R., Blondin, J. M., & Pollock, A. M. T. 1992, ApJ, 386, 265
Torres, A. V., Conti, P. S., & Massey, P. 1986, ApJ, 300, 379
Uesugi, A., & Fukuda, I. 1982, Revised Catalogue of Stellar Rotational Velocities (Kyoto: Kyoto University)
Usov, V. V. 1990, Ap&SS, 167, 297
———. 1991, MNRAS, 252, 49
———. 1992a, ApJ, 389, 635
———. 1992b, in preparation
Usov, V. V., & Melrose, D. B. 1992, ApJ, 395, 575
Volk, H. J., & Biermann, P. L. 1988, ApJ, 333, L65
Weber, E. J., & Davis, L., Jr. 1967, ApJ, 148, 217
White, R. L. 1985, ApJ, 289, 698
White, R. L., & Becker, R. H. 1982, ApJ, 262, 657
———. 1983, ApJ, 272, L19
Williams, P. M., & Eenens, P. R. J. 1989, MNRAS, 240, 445
Williams, P. M., van der Hucht, K. A., Pollock, A. M. T., Florkowski, D. R., van der Woerd, H., & Wamsteker, W. M. 1990, MNRAS, 243, 662
Williams, P. M., van der Hucht, K. A., & Thé, P. S. 1987, A&A, 182, 91
Willis, A. J. 1982, MNRAS, 198, 897
Wright, A. E., & Barlow, M. J. 1975, MNRAS, 170, 41